Since January 2020 Elsevier has created a COVID-19 resource centre with free information in English and Mandarin on the novel coronavirus COVID-19. The COVID-19 resource centre is hosted on Elsevier Connect, the company's public news and information website.

Clinical Immunology 237 (2022) 108981

Contents lists available at ScienceDirect

Clinical Immunology

journal homepage: www.elsevier.com/locate/yclim

Equine immunoglobulin fragment F(ab')$_2$ displays high neutralizing capability against multiple SARS-CoV-2 variants

Divya Gupta [a], Farhan Ahmed [b], Dixit Tandel [a,e], Haripriya Parthasarathy [a], Dhiviya Vedagiri [a,e], Vishal Sah [a,e], B. Krishna Mohan [c], Rafiq Ahmad Khan [b], Chiranjeevi Kondiparthi [c], Prabhudas Savari [c], Sandesh Jain [c], Shashikala Reddy [d], Jerald Mahesh Kumar [a], Nooruddin Khan [b,*], Krishnan Harinivas Harshan [a,e,*,1]

[a] Centre for Cellular and Molecular Biology, Hyderabad 500007, Telangana, India
[b] School of Life Sciences, Department of Animal Biology, University of Hyderabad, Hyderabad 500046, Telangana, India
[c] VINS Bio Products Limited, Hyderabad 500034, Telangana, India
[d] Department of Microbiology, Osmania Medical College, Koti, Hyderabad 500096, Telangana, India
[e] Academy for Scientific and Innovative Research (AcSIR), Ghaziabad 201002, India

ARTICLE INFO

Keywords:
COVID-19
SARS-CoV-2
Antisera
Passive immunotherapy
F(ab')$_2$
Virus neutralization

ABSTRACT

Neutralizing antibody-based passive immunotherapy could be an important therapeutic option against COVID-19. Herein, we demonstrate that equines hyper-immunized with chemically inactivated SARS-CoV-2 elicited high antibody titers with a strong virus-neutralizing potential, and F(ab')$_2$ fragments purified from them displayed strong neutralization potential against five different SARS-CoV-2 variants. F(ab')$_2$ fragments purified from the plasma of hyperimmunized horses showed high antigen-specific affinity. Experiments in rabbits suggested that the F(ab')$_2$ displays a linear pharmacokinetics with approximate plasma half-life of 47 h. *In vitro* microneutralization assays using the purified F(ab')$_2$ displayed high neutralization titers against five different variants of SARS-CoV-2 including the Delta variant, demonstrating its potential efficacy against the emerging viral variants. In conclusion, this study demonstrates that F(ab')$_2$ generated against SARS-CoV-2 in equines have high neutralization titers and have broad target-range against the evolving variants, making passive immunotherapy a potential regimen against the existing and evolving SARS-CoV-2 variants in combating COVID-19.

1. Introduction

COVID-19 caused by severe acute respiratory syndrome coronavirus-2 (SARS-CoV-2) has resulted in over 377 million infections with more than 5.6 million deaths globally as of February 2022 [1]. Though several vaccines have been approved for immunization, it would require years of continuous vaccination drive before we defeat the disease [2,3]. Remdesivir is an antiviral drug used for treating COVID-19, though with limited efficacy [4]. The long delay in vaccination programs coupled with the unavailability of effective drugs and emergence of new variants indicates that COVID-19 is far from being over [5–7]. The situation calls for multiple approaches in countering the viral spread.

Neutralizing antibody (nAb)-based passive immunotherapy has been used as an antiviral therapy module against various intractable viral diseases [8] by blocking the viral attachment and entry into the host cell. Convalescent plasma from the recovered patient has been used as an emergency treatment plan for COVID-19 [9]. However, its scope is limited due to the lack of abundant and reliable blood source, heterogeneous antibody titer, and possible risks of transmission of blood-borne infections [7,10]. Antisera with improved efficacy purified from hyper-immunized equines are a good alternative to convalescent plasma [11,12], but they carry the risk of antibody-dependent enhancement of infection (ADE) and serum sickness [13–16] mostly due to the presence of a constant region (Fc) that allows non-neutralizing antibody attached to the virus to enter cells expressing FcγR [17]. To overcome these limitations, next-generation passive immunotherapy uses the F(ab')$_2$ fragment of antigen-specific immunoglobulins by removing the Fc region of the antibody [18–24].

* Corresponding authors.
E-mail address: hkrishnan@ccmb.res.in (K.H. Harshan).
[1] Lead author

https://doi.org/10.1016/j.clim.2022.108981
Received 8 November 2021; Received in revised form 2 February 2022; Accepted 12 March 2022
Available online 17 March 2022

Based on the above background, we have developed equine SARS-CoV-2 specific immunoglobulin fragment $F(ab')_2$ and evaluated its virus neutralization potential. In this process, equines were immunized with chemically inactivated SARS-CoV-2 particles. The immunoglobulin fragments $F(ab')_2$ prepared from the hyper-immunized equines demonstrated high efficacy of neutralization of multiple SARS-CoV-2 variants. This strategy is reproducible, easily scalable, can be made adaptable against emerging variants, and could be made available for the masses. This approach of immunotherapy will considerably help in managing the global COVID-19 pandemic scenario.

2. Materials and methods

2.1. Cell culture

Vero (CCL-81) cells were cultured in Dulbecco's modified eagle medium (DMEM,

Gibco) supplemented with 10% FBS (Hyclone) and 1 × Penicillin-Streptomycin cocktail (Gibco). Caco2 cells were cultured similarly, but with 20% FBS. Cells were continuously passaged at 70–80% confluency and were maintained in a humidified cell culture incubator at 37 °C and 5% CO_2.

2.2. SARS-CoV-2 propagation, quantification, and infection

All experiments pertaining to the virus isolation and culturing were performed in the biosafety level-3 (BSL-3) laboratory at the Centre for Cellular and Molecular Biology (CCMB). SARS-CoV-2 virus was isolated

from COVID-19 patient samples as reported previously [25]. Briefly, viral transport media (VTM) with lower Ct values (<20) for SARS-CoV-2 genes in real-time qRT-PCR were identified for culturing. Vero cell monolayers in 96 well plates were infected with filter-sterilized VTM. The wells were observed daily for cytopathic effect (CPE). After the appearance of CPE, the supernatants of the corresponding wells were transferred to fresh monolayers of Vero cells and the culture was continued until the viral cultures produced a Ct value of less than 20 and infectious titer in the order of 10^7 mL^{-1}. After the cultures were established, the respective viral genomes were sequenced using next-generation sequencing. Accession IDs for the five variants (B.6, B.1.1.8, B.1.36.29, B.1.1.7 (Alpha), and B.1.617.2 (Delta)) that were used in this study are given in Table 1.

Caco2 or Vero cells grown to 90% confluency were infected with SARS-CoV-2 variants at 1 MOI. 3 h post infection (hpi) in serum-free media, the inoculum was replaced with growth media. The cultures were continued until 48 hpi, when the cells were harvested and processed for immunoblotting.

2.3. Real-time quantification and plaque forming assay

RNA was isolated using viral RNA isolation kit (MACHEREY-NAGEL GmbH & Co. KG). Real-time quantitative RT-PCR was performed in Roche LightCycler 480 either using a commercial kit (LabGun™ COVID-19 RT-PCR Kit) or following WHO guidelines using SuperScript™ III Platinum™ One-Step qRT-PCR Kit (Thermo Fisher Scientific) and TaqMan probes against SARS-CoV-2 *E*- and RdRp (Eurofins Scientific). Raw Ct values generated post analysis of qRT-PCR was used to score the supernatants. For plaque assay, 0.35 million Vero cells were seeded in 6 well plates and serial dilutions of virus supernatants [10–3 to 10–8] were used for infection in serum-free media. Two hpi, cells were briefly washed with 1× PBS to remove unbound virus and overlaid with 1× agarose overlay media (2 × DMEM, 5% FBS, 1% penicillin-streptomycin, 2% LMA). Plates were left undisturbed at 37 °C with 5% CO_2 in an incubator for 6–7 days. Later, 4% formaldehyde in 1 × PBS was added onto the overlay media for fixation and incubated for 15–20 min at 37 °C. The overlay media along with formaldehyde were removed, the cells were washed briefly with 1 × PBS and then stained with crystal violet stain (1% crystal violet in ethanol was used as the stock solution and 0.1% working solution was prepared in double distilled water). The plates were washed, dried and the number of clear zones in the plate was counted to determine the infectious titer as PFU/mL.

Table 1
Description of the variants of SARS-CoV-2 used in this study.

S. No.	Variant	GISAID	Accession number
1.	B.6	hCoV-19/India/TG-CCMB-O2-P1/2020	EPI_ISL_458075
2.	B.1.1.8	hCoV-19/India/TG-CCMB-L1021/2020	EPI_ISL_458046
3.	B.1.36.29	hCoV-19/India/TG-CCMB-AC511/2020	EPI_ISL_539744
4.	B.1.1.7 (Alpha)	hCoV-19/India/TG-CCMB-BB649-P1/2020	EPI_ISL_1672391.2
5.	B.1.617.2 (Delta)	hCoV-19/India/TG-CCMB-CIA4413/2021	EPI_ISL_2775201

2.4. Virus inactivation

The cell culture supernatant of the B.6 isolate containing SARS-CoV-2 was inactivated using beta propiolactone (BPL; HiMedia) at a ratio of 1:2000 following the method reported previously [25] After adding BPL to virus supernatants, the mixture was incubated at 4 °C for 16 h with constant stirring, followed by 4 h incubation at 37 °C to hydrolyze the remaining BPL in the solution. The inactivation of the virus was confirmed by plaque assay or CPE for three consecutive rounds. The absence of plaques or CPE in the lowest dilution confirmed the total inactivation. The BPL treated supernatants were precipitated by ultra-centrifugation and the antigenic integrity of the samples was confirmed by immunoblotting.

2.5. Immunoblotting

Infected cell lysates and virus supernatants were separated on SDS-PAGE gels to confirm the presence and integrity of viral proteins. All samples were lysed in a mild lysis buffer (Tris-Cl, NaCl, NP40; protease and phosphatase inhibitors as mentioned previously [25] and Laemmli loading dye was added. Once the proteins were separated on the gels, they were transferred onto PVDF membranes for 2 h and subsequently blocked in 5% BSA. Blots were probed with Nucleocapsid (Thermo Fisher Scientific; 1:8000) and Spike (Novus Biologicals; 1:2000) primary antibodies followed by HRP-conjugated secondary antibodies and imaged on a Bio-Rad Chemidoc MP system. Image processing was performed using ImageJ [26].

2.6. Mass spectrometry

The viral supernatant proteome was analyzed by protocol adapted a previous report [27]. Briefly the viral supernatant from B.6 variant was concentrated 10 × using 30 kDa centricon filters, then boiled with an equivalent amount of Laemmli buffer and separated on a 12% SDS-PAGE until the protein marker completely entered the resolving gel. Gel sections containing the protein bands were excised, washed, vacuum dried, and subsequently treated with trypsin (15 ng/μL in 25 mM ammonium bicarbonate, 1 mM $CaCl_2$; sequencing grade; Thermo Fisher Scientific) at 37 °C for 16 h. Later, the peptides were extracted using C18 Ziptips (Merck, ZTC18M960). The samples were run on the Q Exactive HF (Thermo Fischer Scientific) to perform HCD mode fragmentation and LC–MS/MS analysis. After the runs were completed, the raw data files were imported into the Proteome Discoverer v2.2 (Thermo Fischer Scientific), analyzed and searched against the UniProt databases of SARS-CoV-2 and *Chlorocebus sabaeus* using the SEQUEST HT algorithm

considering 2 unique peptides. The total peptide count representing both viral and Vero proteomes was normalized against the total number of proteins discovered in the mass spectrometry analysis and was used to plot the graph.

2.7. Equine immunization

Separate groups (lots) each comprising of ten equines were formed and each lot was assigned a unique lot number. These unique numbers were used across the entire study involving activities such as immunization, bleeding and plasmapheresis. The immunization schedule comprised of primary immunization with 1×10^7 inactivated virus particles mixed with Freund's complete adjuvant (FCA) while the subsequent booster immunizations with 1×10^7 inactivated virus particles were administered with Freund's incomplete adjuvant (FIA) on days 15, 29, 35, and 45 (Fig. 1). The viral supernatants were in serum-free media and hence did not contain albumin, a dominant protein component in the culture supernatants. The inactivated supernatants were passed through a 0.45 μm filter to remove cellular debris. Plasma samples from the immunized animals were tested periodically to estimate the antibody response against SARS-CoV-2 inactivated viral antigen. The highest dilutions of the plasma samples necessary to bind with specificity to viral antigen coated in the micro-titer plate were estimated by ELISA. Once the antibody response in the animals was saturated, they were bled and blood volumes equivalent to 1.5% of the individual body weight were collected in glass containers containing acid citrate dextrose solution (final concentration of 15% in the blood volume) to prevent the coagulation. The supernatant plasma in each of the containers was carefully collected and pooled for further studies.

2.8. Measurement of serum IgG titer

Antigen-specific total IgG was measured by indirect ELISA method. The whole viral antigen was coated in the 96 well plate (Nunc) using bicarbonate coating buffer (pH = 9.5) overnight at 4 °C. The coated plates were washed with washing buffer (0.05% Tween-20 in 1× PBS) and blocked with 4% skimmed milk solution for 2 h at RT followed by three rounds of washing. Sera from control and test group were added in the plate at 1:100 dilutions and incubated for 2 h at RT. Subsequently, the plate was washed four times and incubated with HRP conjugated anti-horse whole IgG secondary antibody (Sigma) for 1 h at RT. After washing the plate five times, TMB substrate was added, the reaction continued for about three minutes, and stopped by addition of 0.2 N H_2SO_4. Absorption maxima were recorded at 450 nm and plotted on the

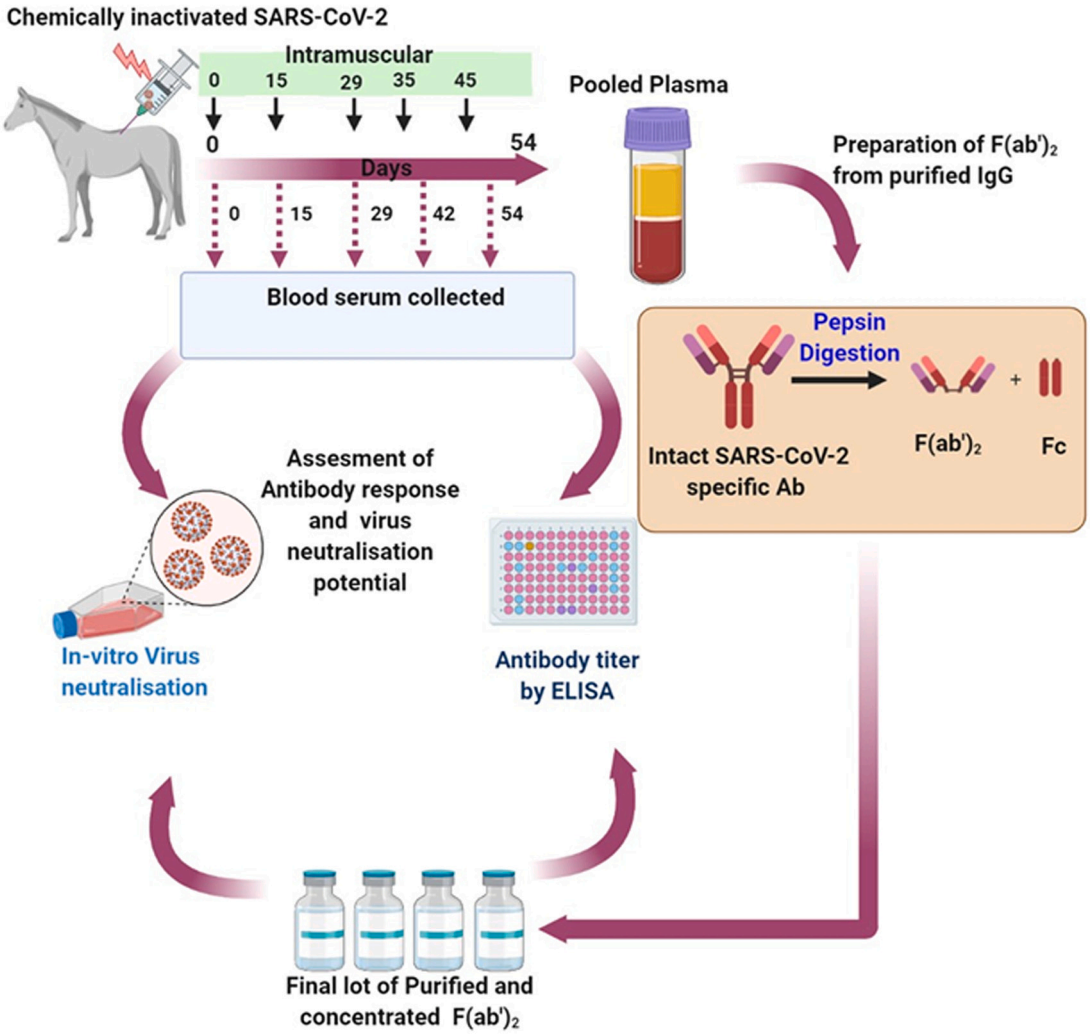

Fig. 1. Immunization scheme and workflow. BPL-inactivated SARS-CoV-2 particles were mixed with FCA and injected intramuscularly into the equines. Immunization was repeated on the days mentioned in the scheme. Plasma collected from the immunized animals were pooled, their antibody response was assayed, and virus neutralization titer was quantified by microneutralization assay. Subsequently, IgG was purified from the pooled plasma, digested with pepsin and the $F(ab')_2$ fragment was purified. Neutralization titers of these purified and concentrated fragments were also assayed.

XY axis graph.

In another set of experiment, $F(ab')_2$ titer kinetics from 0 to 54 days post immunization was calculated by similar ELISA method with slight modification. Here, $F(ab')_2$ samples serially diluted beginning from 1:100 to 1:204800 and added into viral antigen coated plates and ELISA was performed following the protocol mentioned above. Antibody titers were calculated by the reciprocal value of highest dilution at which absorbance value is $\geq$ twice the value of negative control in the same dilution series based on the earlier report [28].

2.9. Virus Neutralization assay

Neutralization capacities of the antisera and $F(ab')_2$ were measured by microneutralization assay in 96-well plates. For neutralization of virus by equine antisera, 30,000 cells were seeded in each well of a 96 well plate 12 h before assay set up. 25 μL of serum-free media containing 300 infectious SARS-CoV-2 particles were mixed with 25 μL of antiserum: serum-free media mix prepared separately. This mix contained antisera at 1:2, 1:4, 1:8 and up to 1:4096 parts of concentrations. The antisera: virus mixes were pre-incubated at 37 °C for 1 h before infection. Subsequently, the wells containing cells were washed with 1 × PBS and the mixes were added to the corresponding wells. After the initial adsorption for 2 h at 37 °C and 5% CO_2, the virus containing media was replaced with fresh serum-sufficient media and incubated for six days. CPE developed in the wells were noted, and the wells were fixed with 100 μL of 4% formaldehyde at 37 °C for 20 min. Post-fixation, formaldehyde was removed, wells were washed and stained with 0.1% crystal violet for 5 min to detect the live cells. The wells were observed against white light and scored for the presence or absence of CPE and CCID 50 was calculated by a modified Reed and Muench formula. The proportionate distance (PD) was first calculated using the formula (% positive above 50%–50%)/ (% positive above 50%- % positive below 50%). The PD obtained was multiplied by the dilution below 50% and value obtained was added to the dilution below 50% to reach the dilution of CCID50).

2.10. Preparation of $F(ab')_2$ immunoglobulin

Thirty liters of pooled plasma was subjected to enzymatic hydrolysis of IgG using pepsin (2% *w/v*) for 2 h with the pH adjusted to 3.3. The enzymatically treated plasma was subjected to complement inactivation by holding at a temperature of 56 °C for 30 mins. Further, caprylic acid was added gradually to make a final concentration of 5% *v*/v and mixed for 1 h. Caprylic acid precipitates non-IgG proteins keeping the $F(ab')_2$ in solution. The antibody fragment $F(ab')_2$ in the supernatant was diafiltered and concentrated by ultrafiltration through a 30 kDa cut-off membrane using 20 mM sodium acetate buffer with 0.9% sodium chloride. The resultant purified concentrated bulk, the key intermediate, was tested for *in vitro* potency by ELISA and viral neutralization by the cell culture method. The concentrated bulk was formulated and filled as a final injectable dosage form, keeping the fill volume to 3 mL per vial. The finished product is intended for administration through either intramuscular or intravenous route based on the severity of the viral load and the urgency of the intervention. Immunization schedule along with the workflow is given in Fig. 1.

2.11. Pharmacokinetics study of $F(ab')_2$

Single dose intravenous pharmacokinetic study of equine anti-SARS-CoV-2 $F(ab')_2$ was performed in 9 male New Zealand white rabbits. The rabbits were divided into three groups with three animals each. G1 group was injected with $F(ab')_2$ at a dose of 3.08 mg/kg body weight while G2 and G3 were injected at 9.24 mg/kg and 30.8 mg/ kg body weight respectively. Dose volume calculated as per body weight of rabbits was administered by slow intravenous injection through the marginal ear vein. The test item was formulated with normal saline. Peripheral blood samples were collected at 0-, 5-, 15- and 30- min and 1-, 2-, 4-, 8-, 12-, 24-, 48-, 72-, 96- and 120 h post-administration and plasma were separated from the blood samples. The samples were analyzed by ELISA with the plates coated with receptor binding domain protein (RBD) to detect the RBD-specific $F(ab')_2$ present in the sample. The bound antibody fragments were detected using a secondary antibody anti-equine goat IgG conjugated with HRP. The A_{450} that is equivalent protein concentration (ng/mL) was calculated from the standard graph and was multiplied with dilution factor to measure the concentration of anti-RBD protein in μg/mL in plasma samples of rabbits in all the three groups. The average $F(ab')_2$ concentrations from the 3 rabbits of each group were calculated for all the samples drawn at varying intervals of time. The Plasma concentrations against the respective time of sampling were tabulated and the data was analyzed by Phoenix WinNonlin 8.3 software (Certara USA) for non-compartmental analysis and calculating the Pharmacokinetic parameters.

2.12. Institutional ethics clearance

Institutional human ethics clearance (IEC-82/2020) was obtained for the patient sample processing for virus culture.

2.13. Institutional animal ethics clearance

Animal experiments were approved by the Institutional Animal Ethics Committee of VINS and CCMB strictly performed according to the guidelines of the Committee for the Purpose of Control and Supervision of Experiments on Animals (CPCSEA).

2.14. Biosafety clearance

SARS-CoV-2 isolation and culturing was approved by the Institutional Biosafety Committee of CCMB. Injection of inactivated SARS-CoV-2 into equines was approved by the Institutional Biosafety Committee of VINS.

3. Results

3.1. Isolation of SARS-CoV-2 particles and establishment of virus culture

Five viral isolates used in this study have been described in Table 1. They included members from B.6 [25], B.1.1.8, B.1.36.29, B.1.1.7 (Alpha), and B.1.617.2 (Delta) variants. To verify the presence of SARS-CoV-2, we analyzed the presence of virion proteins in the supernatants. Detection of spike (S) and nucleocapsid (N) proteins of SARS-CoV-2 in the concentrated viral supernatants confirmed the presence of the virus (Fig. 2A). Immunoblot analysis of SARS-CoV-2 infected Vero cells detected the robust expression of S and N proteins as well (Fig. 2B). We then examined the inactivation of the virus by β-propiolactone (BPL). We used either 1:250 or 1:1000 dilutions of BPL (*v*/v in media) in this study, both of which displayed total inactivation of the virus (data not shown). Detection of viral proteins S and N confirmed the retention of the protein integrity of the inactivated viral stocks to induce immune response in the equines (Fig. 2C). Viral supernatants were subjected to mass spectrometry for analyzing the proportion of viral proteins and the possible presence of Vero proteins in the viral supernatant. The results identified that S and N represented the largest fractions in the supernatants that also contained Vero proteins, but in significantly less proportion (Fig. S1).

3.2. Antigen-specific immune response

The horses were injected with inactivated B.6 variant cultures of SARS-CoV-2 and blood samples were collected periodically (Fig. 1). Plasma prepared from individual animals were subjected to ELISA to

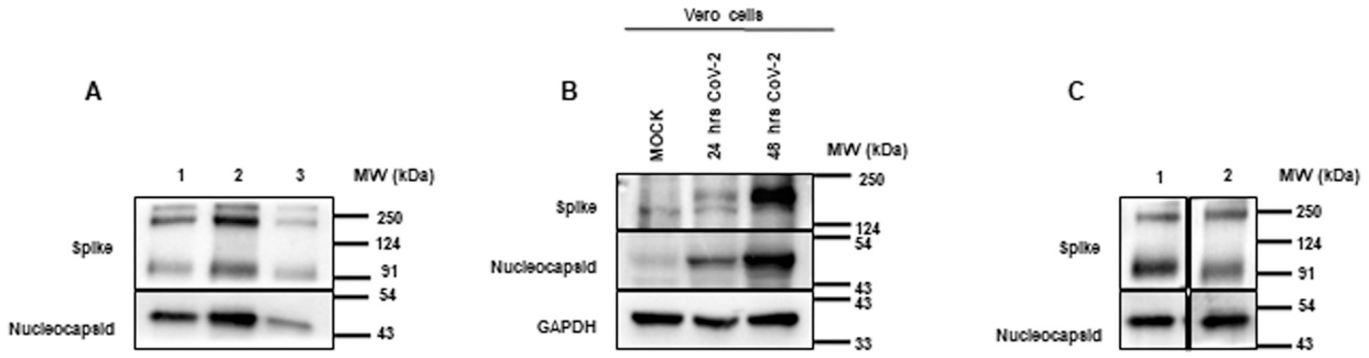

Fig. 2. Characterization of SARS-CoV-2 isolate supernatant and *in vitro* infection. (A) Immunoblotting of SARS-CoV-2 S and N proteins in three independent supernatants from *in vitro* cultures of Vero cells. Briefly, Vero cells were infected with SARS-CoV-2 stocks at 1:10 dilution and three days later supernatants were collected. 10 mL of three independent supernatants were ultra-centrifuged at 100000 ×*g* for 90 min and the pellets were re-suspended in 1 mL of PBS, lysed with 2 × lysis buffer, and immunoblotted. Results from three independent supernatants are depicted. (B) Expression of S and N proteins in Vero cells infected with SARS-CoV-2. The cells were harvested either at 24 or 48 h post-infection before subjecting to immunoblotting. (C) Detection of S and N in BPL-treated viral supernatants. The supernatants were precipitated as in (2A) after the inactivation with BPL. Two individual samples were processed for immunoblotting.

quantify IgG levels. Inactivated viral antigens induced strong IgG response from 15th day onwards peaking at 42 days after priming and subsequently stabilizing as shown in Fig. 3A. Notably, 80% of the immunized horses showed the seroconversion from 29th day onwards except two animals which remained non-responsive during the entire period of study (Fig. 3B). The antibody titer also enhanced from 29th day (1: 25600 dilution) as compared to the negative control, peaking at 42nd day post immunization (1:51200) and later retreating to 1: 25600 at 54th day as demonstrated in Figs. 4 A and B.

3.3. Characterization of $F(ab')_2$ and measurement of their binding titer

Pepsin treatment of the purified IgG-generated **$F(ab')_2$** fragments and the purified **$F(ab')_2$** fraction showed the characteristic peak in the chromatogram (Fig. 5A) with a typical band visible around 110 kDa region in the non-reducing condition and 25 kDa in the reducing condition (Fig. 5B), demonstrating the purity of $F(ab')_2$ preparation. In the non-reducing and reducing condition, $F(ab')_2$ typically shows single band at ~110 kDa and 25 kDa position respectively whereas whole immunoglobulin shows a single band at 150 kDa in non-reducing condition and two bands at 50 kDa (heavy chain) and 25 kDa (light chain) positions under reducing condition. This result confirms that immunoglobulin has been successfully converted into $F(ab')_2$ fragments. Further, immunoblotting of the protein lysates from Caco2 cells infected with five distinct variants of SARS-CoV-2 by purified $F(ab')_2$ identified both S and more strongly N proteins (Fig. 5C), indicating high binding specificity of $F(ab')_2$ to these structural proteins. Next, we measured the titer of the purified **$F(ab')_2$.** The purified **$F(ab')_2$ samples** showed a remarkable titer of 1:102400 as compared to the negative control (Fig. 6).

3.4. Neutralization of SARS-CoV-2 by antisera and purified $F(ab')_2$

We first measured the neutralization potential of plasma from days

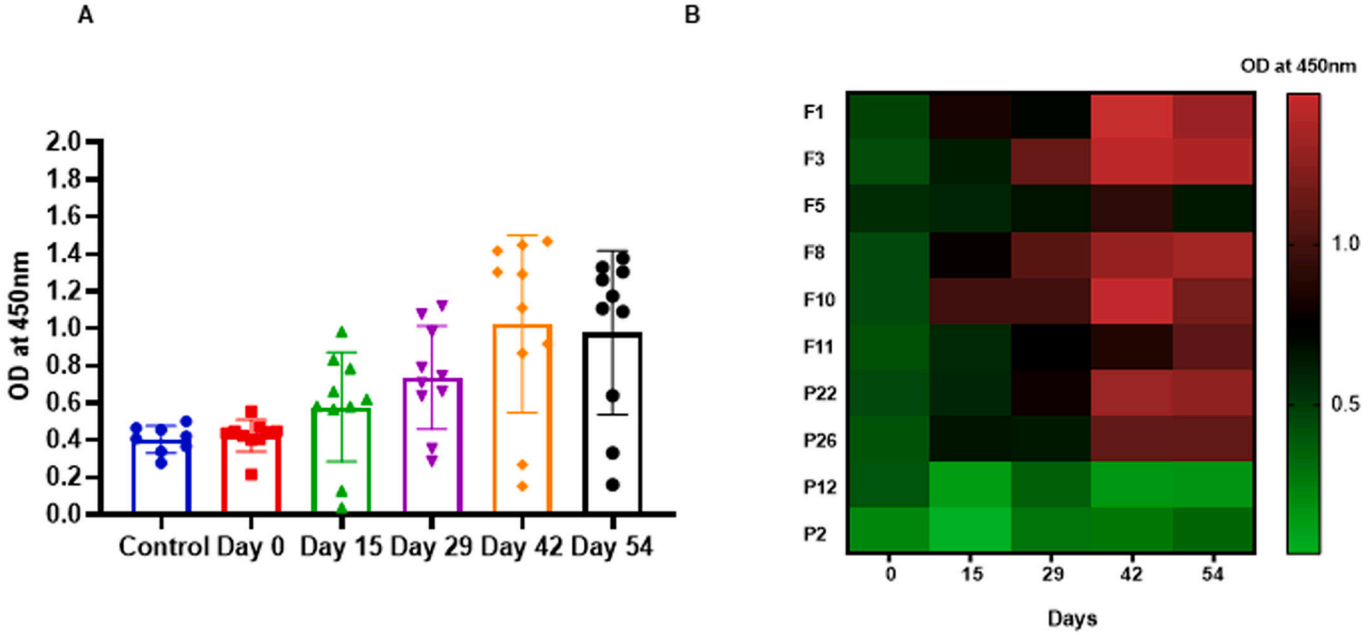

Fig. 3. Evaluation of SARS-CoV-2 specific total IgG from serum collected at specified time points after first immunization using indirect ELISA. (A) Antigen response kinetics of 10 individual horses along the course of time (Day 0 to day 54) with respect to control (pre-immunized sera). (B) Heat map of the same with labeled individual animal.

A

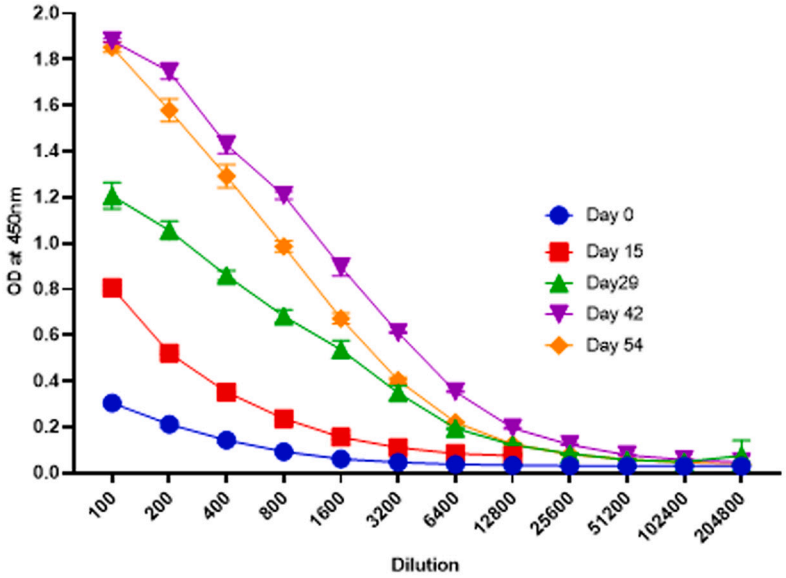

B

Group	Titer
Day 15	6400
Day 29	25600
Day 42	51200
Day 54	25600

Fig. 4. Antibody titration kinetics of serum collected along the different time points using indirect ELISA. (A) Serially diluted serum (1: 100 to 1: 204800) used over the virus antigen coated ELISA plate and absorbance value at each dilution and time points represented at Y axis. (B) Antibody titers were calculated by the reciprocal value of highest dilution at which absorbance value is ≥ twice the value of negative control in the same dilution series.

29, 42 and 54 against B.6 variant. As demonstrated in Fig. 7A, the antisera from three independent time points displayed significantly higher neutralization capacity over the control sera by 29 days post-immunization and spiked at 42 days post-immunization. Next, we assayed the neutralization potencies of purified $F(ab')_2$ by micro-neutralization assay. The purified $F(ab')_2$ generated against B.6 variant demonstrated reasonably high neutralization titer against five distinct variants including the most infectious Delta variant (B.1.617.2) containing D614G mutation in Spike, indicating the efficacy of polyclonal antisera against other variant isolates of SARS-CoV-2 (Fig. 7B). The highest neutralization was detected against the parental B.6 and B.1.36.29 cultures followed by B.1.1.8. Even though $F(ab')_2$ neutralized B.1.1.7 (Alpha), and B.1.617.2 (Delta) at lower efficiency, the neutralization titers are still significant enough at 8192. Cross neutralizing ability of antisera reduces the risk burden of its therapeutic relevance against emerging SARS-CoV-2 variants, thereby suggesting that the equine-purified $F(ab')_2$ based passive immunotherapy holds enormous therapeutic potential against COVID-19 in terms of cost, safety, storage and mass availability.

3.5. *Pharmacokinetics study of F(ab')$_2$*

As described in the Methods, we used three different doses of $F(ab')_2$ in rabbits with the G1, G2 and G3 receiving $F(ab')_2$ at a dose of 3.08, 9.24 and 30.8 mg/kg body weight respectively. C_{max} was achieved across the groups in 5 mins after administration (Table 2). The mean C_{max} observed in low, medium and high dose was 37.21 μg/mL, 69.52 μg/mL, and 88.67 μg/mL respectively. The derived plasma half-life ($T_{1/2}$) of the equine antibody fragments was observed to be 47.7 h for low dose (3.08 mg/kg), 47.4 h for the mid dose (9.24 mg/Kg) and 70.15 h for the high dose (30.8 mg/kg) (Table 2). Area under curve (AUC) for the low, mid and high dosing group was found to be 1041, 2598 and 5073 μg*hr/ml respectively which shows the drug distribution with function of time. These results indicate that the $F(ab')_2$ has a robust bioavailability that would be important in the effective neutralization of SARS-CoV-2 in the clinical set up.

4. Discussion

Emerging and re-emerging zoonotic viral infectious diseases such as SARS-CoV-2, SARS-CoV and MERS-CoV have become more frequent in the recent past due to the ever-increasing encounters with wild animals and pose great threat to public health system. Several vaccines have been introduced into the markets and they are reported to be quite effective while some of them have been approved for emergency use [3,29]. Antibody therapy holds important position in the fight against COVID-19 since vaccinating the entire human population would require years of continuous vaccination. Several monoclonal antibodies (mAbs) have shown their neutralization potential against SARS-CoV-2 [30,31], but production of individual mAbs are resource-exhaustive and also bear the risk of losing their potential against the possible mutants in the specific epitopes [32,33]. Polyclonal antibodies generated in large animals such as equines have the advantage of faster generation, requirement of relatively much smaller investment and efficacy against multiple epitopes [22,23]. Antisera generated from such sources had been a great source of antiviral antibody to treat the various viral infection such as SARS-CoV, Ebola, MERS-CoV and avian influenza virus [34–37]. Clinical evidence of COVID-19 disease shows that latent period of infection is short and majority of the patients recover faster without any persistent infection thus increasing the prospects of using neutralizing antibodies in blocking the SARS-CoV-2 virus particles [38]. Even though convalescent plasma from the recovered patients was considered to be a great source of neutralizing antibodies [39], the difficulty in recruiting such individuals along with the lack of consistency in the neutralizing antibody titer among them has posed major obstacles in utilizing its potential [40]. Moreover, several reports indicate the lack of efficacy of convalescent plasma therapy in improving the severity of COVID-19 [41,42]. Notwithstanding the use of plasma therapy to treat various infectious viral disease such as SARS, H5N1 and Ebola [35,43,44] it always carries a risk of blood-borne infection and its limited availability hampers its prospect of universal application.

Considering the enormous potential of antibody based therapy, we developed SARS-CoV-2 specific immunoglobulin fragments $F(ab')_2$ in equines using chemically inactivated virus as similar to other reported

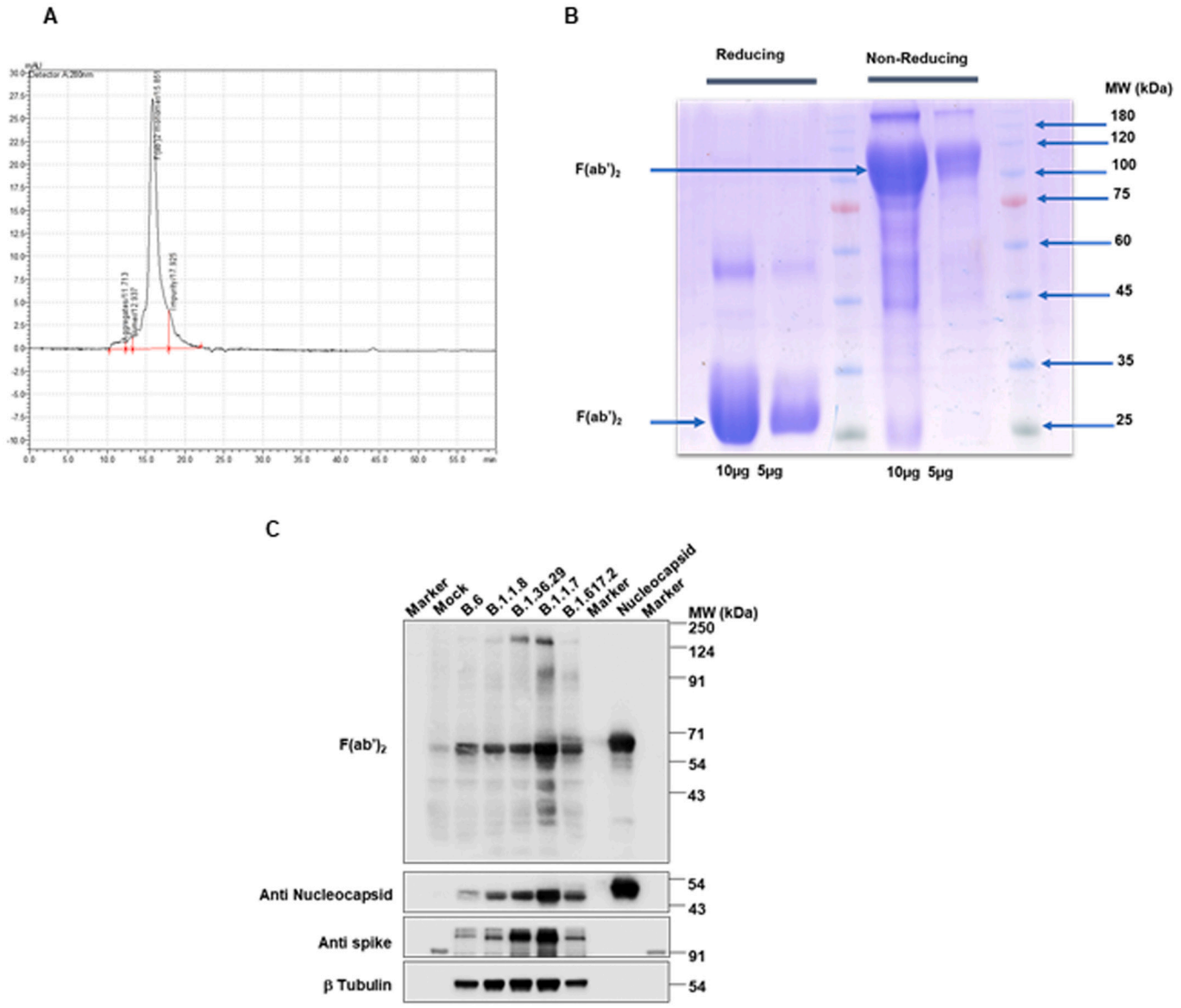

Fig. 5. Characterization of purified F(ab')$_2$. (A) HPLC chromatogram shows a dominant F(ab')$_2$ peak (B) SDS-PAGE image of purified F(ab')$_2$ under reducing and non-reducing conditions. The purified F(ab')$_2$ were loaded (5 or 10 µg) with and without β-mercaptoethanol in SDS-polyacrylamide gel and resolved under constant voltage. The result shows F(ab')$_2$ fragment of 25 kDa (two heavy chains and two light chains of almost similar molecular weight) under reducing condition (left) and $>$ 110 kDa under non-reducing condition (right) demonstrating the purity of F(ab')$_2$ preparation. (C) The affinity of pure F(ab')$_2$ for its antigen was determined using Immunoblotting. SARS-CoV-2-infected Caco2 cell lysates were electrophoresed on reducing SDS-PAGE, immunoblotted, and probed with pure F(ab')$_2$, and specific binding of F(ab')$_2$ was assessed using an anti-horse anti-F(ab')$_2$-HRP secondary antibody. S and N expression were also detected using specific antibodies. Purified recombinant N was also electrophoresed as a positive control.

work [11,35]. F(ab')$_2$ that we generated achieved greater antigen specific antibody titer of 1: 102400 which is comparatively better than the earlier published reports [34,35]. Other recent reports also demonstrated high antibody titer for F(ab')$_2$ generated from horses using receptor binding domain (RBD) of spike protein [17,18,23]. One of these studies reported clinical efficacy of F(ab')$_2$ [24] while another one has reported results from challenge studies in hamsters [18]. These studies used Spike or its RBD as antigen. Study by Cunha et al., also demonstrated the potency against Gamma [18]. However, in our study, we used inactivated whole virus as the antigen and the potency was tested against five distinct variant isolates including Delta. Generation of inactivated virus was a more direct and feasible approach for us than raising large amounts of vaccine quality spike proteins to be used at commercial levels. Apart from the lesser side effect, F(ab')$_2$ can penetrate deeper into the organs due to smaller size and lesser cellular affinity therefore it can neutralize the virus in the extravascular tissue [46].

F(ab')$_2$ also demonstrated robust *in vitro* virus neutralization titer which is comparable with other similar studies against the SARS-CoV-2 [17,18,20,33,45,47]. These studies have primarily relied on recombinant viral protein(s) as the immunogen. Effective neutralization of SARS-CoV-2 variants carrying distinct mutations in spike protein, including the Delta variant by a formulation of purified F(ab')2 obtained from horses hyperimmunized with inactivated virus demonstrates the therapeutic potential of this product. Since the dominant variants that emerged during the course of the pandemic had distinct mutations in the S protein, the efficacy of F(ab')$_2$ generated against a particular variant, against the emerging variants was a major concern. Studies using monoclonal antibodies against SARS-CoV-2 showed a lower neutralization efficiency against the dominant B.1.617.2 (Delta) variant

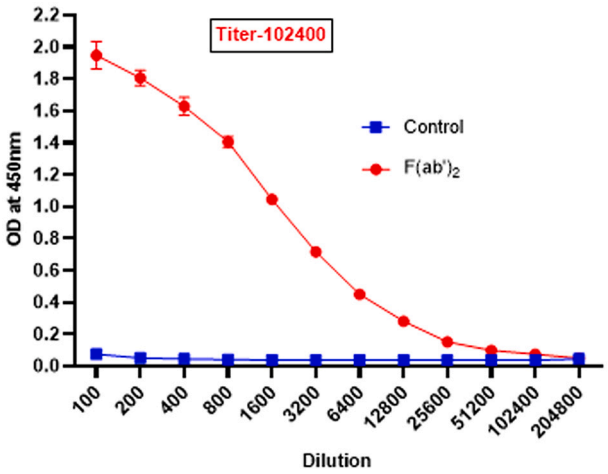

Fig. 6. Antibody titration of the F(ab')$_2$ purified from the pooled plasma of immunized equine with respect to pooled sample of negative control and titer is given in inset box. F(ab')$_2$ titer was measured by direct ELISA method in which the whole virus antigen (approximately 1×10^5 virus particles) coated-plates were incubated with serially diluted F(ab')$_2$ (1:100 to 1:204800 dilution) for 2 h at RT. HRP conjugated anti-F(ab')$_2$ secondary antibody (1:5000 dilution) was added subsequently and the color reaction was developed by adding TMB substrate. F(ab')$_2$ titer was calculated by the reciprocal value of highest dilution at which absorbance value is $\geq$ twice the value of negative control in the same dilution series.

[48,49]. However, our studies demonstrated that the F(ab')$_2$ have comparable binding affinity for the antigen and showed adequate neutralization and hence are of great potential in COVID-19 therapeutics. Another report also demonstrates that formulations of equine hyperimmune antibodies efficiently neutralize several major variants of concern including B.1.617.2 [23], indicating the efficacy of purified equine-derived antibodies in COVID-19 treatment. Furthermore, the F(ab')$_2$ shows very significant virus neutralization that is higher than what the convalescent plasma therapy offers without the risk of blood born disease [50]. The WHO guidelines are already laid out for the production and application of antisera and their product from equine source therefore it can be quickly available to the world for immediate application [51]. Strain-specific antisera can be developed quickly based on the necessity. Even in the optimistic scenario of active vaccines, passive immunotherapy can also be used to save the life of patients several of who would otherwise go to terminal stages, by neutralizing the virus and thereby reducing both mortality and morbidity in COVID-19.

Author contributions

D.G. optimized large-scale SARS-CoV-2 virus propagation, BPL inactivation and microneutralization assay. D.G., and D·K propagated, quantified, and inactivated large-scale SARS-CoV-2 cultures, and performed microneutralization assays. D·V, D.K., and V·S established SARS-CoV-2 cultures used in this study. H.P. performed immunoblotting. N.K. conceived and conceptualized the study along with K.H.H. F.A. and R.K. performed the immunological characterization of anti-sera and F(ab')$_2$. D. G., F.A., K.H.H. and N.K. wrote the manuscript. C.K., P.S., and S.J performed the equine immunization and F(ab')$_2$ preparation. S.D., and J.D provided the logistics for the immunization. J.M.K performed the

Table 2
Single-dose pharmacokinetics study of equine-derived anti-SARS-CoV-2 F(ab')$_2$ performed in rabbits. Animals were grouped and administered three different amounts of F(ab')$_2$ and blood was collected at several time points. Each group consisted of three individual animals. Purified sera were used against RBD in indirect ELISA to measure the bioavailability of the F(ab')$_2$ in the peripheral blood. The plasma concentration against time was tabulated and data was analyzed using Phoenix WinNonlin 8.3 software.

Dose group (mg/kg B.W.)	T1/2 (hrs)	C_{max} (μg/ml)	AUC (hrs*μg/ml)
3.08	47.7471977	37.21	1041.781254
9.24	47.4269128	69.5	2598.287913
30.8	70.1468822	88.97	5073.924194

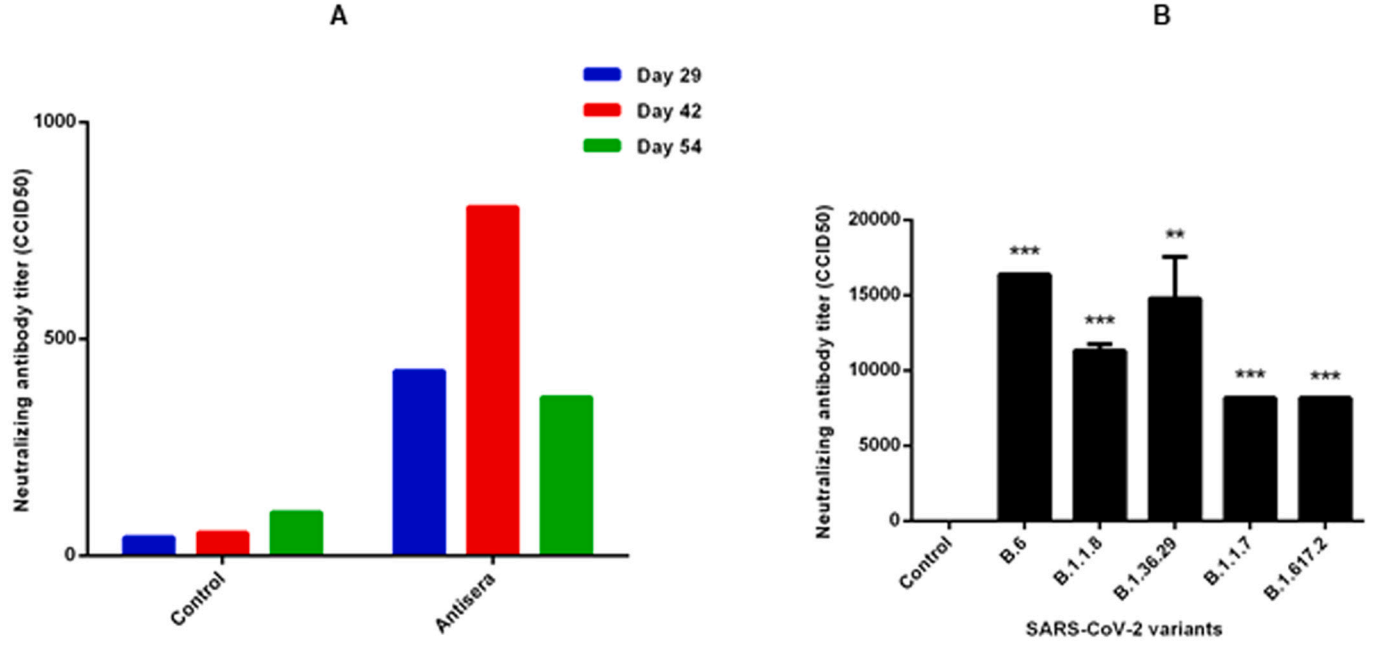

Fig. 7. Neutralization capacities of host antisera and purified F(ab')$_2$. (A) Neutralization of SARS-CoV-2 by pooled of antisera. Neutralization capacities of antisera drawn from horses 29-, 42- and 54-days post-immunization were tested by micro neutralization assays against the parental strain B.6. CCID50 of the antisera treated virus particles are represented. (B) Neutralization capacities of F(ab')$_2$ generated from pooled antisera against different variants of SARS-CoV-2. Micro neutralization assays were performed similarly as in Fig. 6 and the data are represented as CCID50.

pharmacokinetics studies. S.R provided the patient sample for the isolation of SARS-CoV-2.

Declaration of Competing Interest

The authors declare no conflict of interests in this study.

Acknowledgement

This study was supported by internal funding of CSIR-CCMB and funds from VINS to both CSIR-CCMB and University of Hyderabad. Several volunteers at the Centre for Cellular and Molecular Biology who were part of COVID-19 testing are thanked for their help in identifying SARS-CoV-2 positive samples for virus culturing. Mohan Singh Moodu and Amit Kumar contributed significantly with the logistics. We also thank Zeba Rizvi and G. Srinivas Reddy for their assistance in processing and analyzing mass spectrometry data. We thank Karthika Nair, Abhirami P S, and Sai Poojitha for their help with various experiments.

Appendix A. Supplementary data

Supplementary data to this article can be found online at https://doi.org/10.1016/j.clim.2022.108981.

References

[1] World Health Organization (WHO), WHO Coronavirus Disease (COVID-19) Dashboard, 2 February 2022.
[2] WHO, Draft landscape of COVID-19 candidate vaccines-15 October 2020, Who, 2020.
[3] S. Joffe, Evaluating SARS-CoV-2 vaccines after emergency use authorization or licensing of initial candidate vaccines, JAMA - J. Am. Med. Associat. 325 (2021) 221–222.
[4] J.H. Beigel, K.M. Tomashek, L.E. Dodd, A.K. Mehta, B.S. Zingman, A.C. Kalil, et al., Remdesivir for the treatment of Covid-19 — final report, N. Engl. J. Med. 383 (19) (2020) 1813–1826, https://doi.org/10.1056/NEJMoa2007764.
[5] Q.X. Long, X.J. Tang, Q.L. Shi, Q. Li, H.J. Deng, J. Yuan, et al., Clinical and immunological assessment of asymptomatic SARS-CoV-2 infections, Nat. Med. 26 (8) (2020) 1200–1204, https://doi.org/10.1038/s41591-020-0965-6.
[6] A. Casadevall, M.J. Joyner, L.A. Pirofski, SARS-CoV-2 viral load and antibody responses: the case for convalescent plasma therapy, J. Clin. Investig. 130 (10) (2020) 5112–5114, https://doi.org/10.1172/JCI139760.
[7] S. Yin, X. Tong, A. Huang, H. Shen, Y. Li, Y. Liu, et al., Longitudinal anti-SARS-CoV-2 antibody profile and neutralization activity of a COVID-19 patient, J. Inf. Secur. 81 (3) (2020) e31–e32, https://doi.org/10.1016/j.jinf.2020.06.076.
[8] G. Salazar, N. Zhang, T.M. Fu, Z. An, Antibody therapies for the prevention and treatment of viral infections, npj Vaccines. 2 (2017), 19, https://doi.org/10.1038/s41541-017-0019-3.
[9] J.H. Tanne, Covid-19: FDA approves use of convalescent plasma to treat critically ill patients, BMJ. 368 (m1256) (2020), https://doi.org/10.1136/bmj.m1256.
[10] P. Tiberghien, X. de Lamballerie, P. Morel, P. Gallian, K. Lacombe, Y. Yazdanpanah, Collecting and evaluating convalescent plasma for COVID-19 treatment: why and how? Vox Sang. 115 (6) (2020) 488–494, https://doi.org/10.1111/vox.12926.
[11] X. Pan, Y. Wu, W. Wang, L. Zhang, G. Xiao, Development of horse neutralizing immunoglobulin and immunoglobulin fragments against Junín virus, Antivir. Res. 174 (104666) (2020), https://doi.org/10.1016/j.antiviral.2019.104666.
[12] H. Wang, G. Wong, W. Zhu, S. He, Y. Zhao, F. Yan, et al., Equine-origin immunoglobulin fragments protect nonhuman Primates from Ebola virus disease, J. Virol. 93 (5) (2018), https://doi.org/10.1128/JVI.01548-18.
[13] R.E. Black, R.A. Gunn, Hypersensitivity reactions associated with botulinal antitoxin, Am. J. Med. 69 (4) (1980) 567–570, https://doi.org/10.1016/0002-9343(80)90469-6.
[14] F. Luo, F.L. Liao, H. Wang, Tang H. Bin, Z.Q. Yang, W. Hou, Evaluation of antibody-dependent enhancement of SARS-CoV infection in Rhesus macaques immunized with an inactivated SARS-CoV vaccine, Virol. Sin. 33 (2) (2018) 201–204, https://doi.org/10.1007/s12250-018-0009-2.
[15] G. León, M. Herrera, Á. Segura, M. Villalta, M. Vargas, J.M. Gutiérrez, Pathogenic mechanisms underlying adverse reactions induced by intravenous administration of snake antivenoms, Toxicon. 76 (2013 Dec) 63–76.
[16] H.A. De Silva, N.M. Ryan, H.J. De Silva, Adverse reactions to snake antivenom, and their prevention and treatment, Br. J. Clin. Pharmacol. 81 (3) (2016 Mar) 446–452.
[17] D. Li, R.J. Edwards, K. Manne, D.R. Martinez, A. Schäfer, S.M. Alam, et al., In vitro and in vivo functions of SARS-CoV-2 infection-enhancing and neutralizing antibodies, Cell. 184 (16) (2021 Aug) 4203–4219.e32.
[18] L.E.R. Cunha, A.A. Stolet, M.A. Strauch, V.A.R. Pereira, C.H. Dumard, A.M. O. Gomes, et al., Polyclonal F(ab')2 fragments of equine antibodies raised against the spike protein neutralize SARS-CoV-2 variants with high potency, iScience 24 (11) (2021 Nov) 103315.
[19] X. Pan, P. Zhou, T. Fan, Y. Wu, J. Zhang, X. Shi, et al., Immunoglobulin fragment F (ab')2 against RBD potently neutralizes SARS-CoV-2 in vitro, Antivir. Res. 182 (104868) (2020), https://doi.org/10.1016/j.antiviral.2020.104868.
[20] V. Zylberman, S. Sanguineti, A.V. Pontoriero, S.V. Higa, M.L. Cerutti, S.M.M. Seijo, et al., Development of a Hyperimmune equine serum therapy for COVID-19 in Argentina. Buenos Aires 80, 2020, pp. 1–6.
[21] G. León, M. Herrera, M. Vargas, M. Arguedas, A. Sánchez, Á. Segura, et al., Development and characterization of two equine formulations towards SARS-CoV-2 proteins for the potential treatment of COVID-19, Sci. Report. 11 (1) (2021) 1–15.
[22] A. Alape-Girón, A. Moreira-Soto, M. Arguedas, H. Brenes, W. Buján, E. Corrales-Aguilar, et al., Heterologous hyperimmune polyclonal antibodies against SARS-CoV-2: a broad coverage, affordable, and scalable potential immunotherapy for COVID-19, Front Med. 8 (2021 Sep).
[23] A. Moreira-Soto, M. Arguedas, H. Brenes, W. Buján, E. Corrales-Aguilar, C. Díaz, et al., High efficacy of therapeutic equine hyperimmune antibodies against SARS-CoV-2 variants of concern, Front Med. 0 (2021 Sep) 1482.
[24] G. Lopardo, W.H. Belloso, E. Nannini, M. Colonna, S. Sanguineti, V. Zylberman, et al., RBD-specific polyclonal F(ab)2 fragments of equine antibodies in patients with moderate to severe COVID-19 disease: a randomized, multicenter, double-blind, placebo-controlled, adaptive phase 2/3 clinical trial, EClinicalMedicine. 34 (2021 Apr), 100843.
[25] D. Gupta, H. Parthasarathy, V. Sah, D. Tandel, D. Vedagiri, S. Reddy, et al., Inactivation of SARS-CoV-2 by β-propiolactone causes aggregation of viral particles and loss of antigenic potential, Virus Res. (2021 Nov) 305.
[26] C.A. Schneider, W.S. Rasband, K.W. Eliceiri, NIH Image to ImageJ: 25 years of image analysis. Vol. 9, Nat. Methods (2012) 671–675. Nature Publishing Group.
[27] M. Bhattacharjee, N. Adhikari, R. Sudhakar, Z. Rizvi, D. Das, R. Palanimurugan, et al., Characterization of plasmodium falciparum NEDD8 and identification of cullins as its substrates, Sci Rep [Internet]. 10 (1) (2020 Dec 1), 20220, https://doi.org/10.1038/s41598-020-77001-5 [cited 2022 Jan 29];10(1). Available from: https://pubmed.ncbi.nlm.nih.gov/33214620/.
[28] A. Frey, J. Di Canzio, D. Zurakowski, A statistically defined endpoint titer determination method for immunoassays, J. Immunol. Methods 221 (1–2) (1998) 35–41, https://doi.org/10.1016/s0022-1759(98)00170-7.
[29] F.P. Polack, S.J. Thomas, N. Kitchin, J. Absalon, A. Gurtman, S. Lockhart, et al., Safety and efficacy of the BNT162b2 mRNA Covid-19 vaccine, N. Engl. J. Med. 383 (27) (2020 Dec) 2603–2615.
[30] T.F. Rogers, F. Zhao, D. Huang, N. Beutler, A. Burns, W.T. He, et al., Isolation of potent SARS-CoV-2 neutralizing antibodies and protection from disease in a small animal model, Science (80-). 369 (6506) (2020 Aug) 956–963.
[31] J. Wan, S. Xing, L. Ding, Y. Wang, C. Gu, Y. Wu, et al., Human-IgG-neutralizing monoclonal antibodies block the SARS-CoV-2 infection, Cell Rep. 32 (3) (2020 Jul) 107918.
[32] D. Planas, D. Veyer, A. Baidaliuk, I. Staropoli, F. Guivel-Benhassine, M.M. Rajah, et al., Reduced sensitivity of SARS-CoV-2 variant Delta to antibody neutralization, Nat 596 (7871) (2021) 276–280, 5967871.
[33] M. Hoffmann, H. Hofmann-Winkler, N. Krüger, A. Kempf, I. Nehlmeier, L. Graichen, et al., SARS-CoV-2 variant B.1.617 is resistant to bamlanivimab and evades antibodies induced by infection and vaccination, Cell Rep. 36 (3) (2021 Jul) 109415.
[34] Y. Zhao, C. Wang, B. Qiu, C. Li, H. Wang, H. Jin, et al., Passive immunotherapy for Middle East respiratory syndrome coronavirus infection with equine immunoglobulin or immunoglobulin fragments in a mouse model, Antivir. Res. 137 (2017) 125–130, https://doi.org/10.1016/j.antiviral.2016.11.016.
[35] J.H. Lu, Z.M. Guo, W.Y. Han, G.L. Wang, D.M. Zhang, Y.F. Wang, et al., Preparation and development of equine hyperimmune globulin F(ab') 2 against severe acute respiratory syndrome coronavirus, Acta Pharmacol. Sin. 26 (12) (2005) 1479–1484, https://doi.org/10.1111/j.1745-7254.2005.00210.x.
[36] O.V. Pyankov, Y.X. Setoh, S.A. Bodnev, J.H. Edmonds, O.G. Pyankova, S. A. Pyankov, et al., Successful post-exposure prophylaxis of Ebola infected non-human primates using Ebola glycoprotein-specific equine IgG, Sci. Rep. 3 (7) (2017), 41537, https://doi.org/10.1038/srep41537.
[37] C. Bal, C.H. Herbreteau, P. Buchy, S. Rith, M. Zaid, W. Kristanto, et al., Safety, potential efficacy, and pharmacokinetics of specific polyclonal immunoglobulin F (ab')2 fragments against avian influenza a (H5N1) in healthy volunteers: a single-centre, randomised, double-blind, placebo-controlled, phase 1 study, Lancet Infect. Dis. 15 (3) (2015) 285–292, https://doi.org/10.1016/S1473-3099(14)71072-2.
[38] S.A. Lauer, K.H. Grantz, Q. Bi, F.K. Jones, Q. Zheng, H.R. Meredith, et al., The incubation period of coronavirus disease 2019 (CoVID-19) from publicly reported confirmed cases: estimation and application, Ann. Intern. Med. 172 (9) (2020) 577–582, https://doi.org/10.7326/M20-0504.
[39] M. Rojas, Y. Rodríguez, D.M. Monsalve, Y. Acosta-Ampudia, B. Camacho, J. E. Gallo, et al., Convalescent plasma in Covid-19: possible mechanisms of action, Autoimmun. Rev. 19 (7) (2020), 102554, https://doi.org/10.1016/j.autrev.2020.102554.
[40] S.T.H. Liu, H.M. Lin, I. Baine, A. Wajnberg, J.P. Gumprecht, F. Rahman, et al., Convalescent plasma treatment of severe COVID-19: a propensity score–matched control study, Nat. Med. 26 (11) (2020) 1708–1713, https://doi.org/10.1038/s41591-020-1088-9.
[41] A. Agarwal, A. Mukherjee, G. Kumar, P. Chatterjee, T. Bhatnagar, P. Malhotra, Convalescent plasma in the management of moderate covid-19 in adults in India: open label phase II multicentre randomised controlled trial (PLACID trial), BMJ. 371 (2020 Oct).

[42] V.A. Simonovich, L.D. Burgos Pratx, P. Scibona, M.V. Beruto, M.G. Vallone, C. Vázquez, et al., A randomized trial of convalescent plasma in Covid-19 severe pneumonia, N. Engl. J. Med. 384 (7) (2020 Nov) 619–629, https://doi.org/10.1056/NEJMoa2031304. NEJMoa2031304.
[43] S. Rockman, S. Lowther, S. Camuglia, K. Vandenberg, S. Taylor, L. Fabri, et al., Intravenous immunoglobulin protects against severe pandemic influenza infection, EBioMedicine. 19 (2017) 119–127, https://doi.org/10.1016/j.ebiom.2017.04.010.
[44] C.S. Kraft, A.L. Hewlett, S. Koepsell, A.M. Winkler, C.J. Kratochvil, L. Larson, et al., The use of TKM-100802 and convalescent plasma in 2 patients with Ebola virus disease in the United States, Clin. Infect. Dis. 61 (4) (2015) 496–502, https://doi.org/10.1093/cid/civ334.
[45] L.E.R. Cunha, A.A. Stolet, M.A. Strauch, V.A.R. Pereira, C.H. Dumard, P.N. C. Souza, et al., Equine hyperimmune globulin raised against the SARS-CoV-2 spike glycoprotein has extremely high neutralizing titers, bioRxiv. (2020).
[46] A.H. Laustsen, J. María Gutiérrez, C. Knudsen, K.H. Johansen, E. Bermúdez-Méndez, F.A. Cerni, et al., Pros and cons of different therapeutic antibody formats for recombinant antivenom development, Toxicon. 146 (2018) 151–175, https://doi.org/10.1016/j.toxicon.2018.03.004.
[47] Palakurthi Biological Limited KE, Vikram Paradkar Biological Limited HE, H. Priya Abraham, Development of Equine Antisera with High Neutralizing Activity Against SARS-CoV-2, 2020 Sep.
[48] Delphine Planas, David Veyer, Artem Baidaliuk, Isabelle Staropoli, Florence Guivel-Benhassine, Maaran Michael Rajah, et al., Reduced sensitivity of SARS-CoV-2 variant Delta to antibody neutralization, Nature. 596 (7871) (2021 Aug) 276–280.
[49] B. Wang, Y.S. Goh, S.W. Fong, B.E. Young, Ngoh EZX, J.M. Chavatte, et al., Resistance of SARS-CoV-2 Delta variant to neutralization by BNT162b2-elicited antibodies in Asians, Lancet Reg Heal West Pacific. 15 (100276) (2021 Oct).
[50] S. Wendel, J.M. Kutner, R. Machado, R. Fontão-Wendel, C. Bub, R. Fachini, et al., Screening for SARS-CoV-2 antibodies in convalescent plasma in Brazil: preliminary lessons from a voluntary convalescent donor program, Transfusion. 60 (12) (2020) 2938–2951, https://doi.org/10.1111/trf.16065.
[51] World Health Organization (WHO), Guidelines for the production, control and regulation of snake antivenom immunoglobulins, Biol Aujourdhui. (2010).